High Output Dynamic UWB Pulse Generator for BPSK Modulations

E. Muhr, R. Vauche, Sylvain Bourdel, Jean Gaubert, Oswaldo Ramos Sparrow Ramos Sparrow, Nicolas Dehaese, I. Benamor, Herve Barthelemy

High Output Dynamic UWB Pulse Generator for BPSK Modulations

E. Muhr[1], R. Vauche[2], S. Bourdel[1], J. Gaubert[1], O. Ramos Sparrow[1], N. Dehaese[1], I. Benamor[1], H. Barthelemy[3]

[1]Aix-Marseille University, [2]ISEN-Toulon, [3]Toulon University, IM2NP, and CNRS, IM2NP (UMR 7334),
Campus de Saint-Jérôme, Avenue Escadrille Normandie Niemen - Case 142, F-13397 Marseille Cedex, France

***Abstract*— This paper presents the design of a fully integrated pulse generator which allows BPSK modulation to be implemented. This emitter is based on the response filter architecture and has been integrated in a 130nm CMOS technology with a 1.2V supply voltage on a silicon area of 2.88mm². The bandwidth at -10dB is about 1.8GHz around 3.52GHz. The output dynamic voltage is equal to 1.72V peak to peak on a 100Ω differential load which gives an energy of 1.93pJ for the twice bipolar generated pulses and demonstrates the pulse generator capability to be used for bipolar modulations.**

BPSK; Filter Impulse Response; IR-UWB; Pulse Generator.

I. INTRODUCTION

Since 2002, the Federal Communications Commission (FCC) regulated the frequencies from 3.1GHz to 10.6GHz which is called Ultra-Wide Band (UWB). To use this band, 3 rules must be respected: (i) comply with an average Equivalent Isotropic Radiated Power (EIRP) mask having a maximum value equal to -41.3dBm or 50nW on a 50Ω load in 3.1-10.6GHz band when it is measured in a Resolution BandWidth (RBW) of 1MHz, (ii) occupy a minimum BandWidth (BW_{-XdB}) or relative BandWidth ($\%BW_{-XdB}$) defined at -10dB respectively equal to 500MHz or 20%, (iii) generate a maximum Peak Power P_P equal to 0dBm when it is measured in a band of 50MHz around f_M where f_M is the frequency associated to the maximum value of EIRP. These particular specifications allow UWB band to be used by Impulse Radio (IR) which is a promising technology in UWB band (IR-UWB) for communications in short range application thanks to simple architectures that can be used. Moreover, IR-UWB transmitters are low-cost systems since they can be fully integrated [1][2][3], and low-power systems by shutting down transceiver between two consecutive pulses or two bursts [4] since IR-UWB uses short duration pulses.

High output dynamic is an important issue to improve the energy of the emitted pulse in a given bandwidth and then to improve the budget link of a transmission. This is all the more important since IR-UWB is well suited to low cost systems which can use non-coherent detection. Due to the gated nature of an IR-UWB signal, it is possible to increase the energy of the emitted pulse by reducing the bit rate [5]. In such conditions, it is more interesting to use a Binary Phase Shift Keying (BPSK) than an On-Off Keying (OOK) modulation since bipolar modulations (such as BPSK) are not limited by a discrete spectrum. Bipolar modulations are known to allow higher energy pulses to be generated for higher bit rates than OOK and should also be used when an high output dynamic is needed. This energy can be further improved by using Alternate Mark Inversion (AMI) modulation which consists in emitting an UWB pulse when a '1' has to be sent, the opposite of the last emitted pulse when another '1' is emitted, and no pulse when a '0' must be transmitted.

Since UWB pulse generators are an important part of an IR-UWB transceiver, many studies [6][7][8] have been done and demonstrate that an UWB pulse generator can be integrated on a standard CMOS technology which is more suitable for low-cost systems than architectures based for example on Step Recovery Diode [9][10]. In literature, three different CMOS pulse generator architectures are highlighted and can be used in UWB emitters. The first architecture of pulse generator is based on a switched oscillator where the pulse envelop depends on the start conditions of the LO which limits the output dynamic. This limitation increases with the pulse bandwidth which limits the interest of such architecture for bandwidth higher than 2GHz [5]. Another limitation of switched oscillators is that they are difficult to use for bipolar modulations since the starting phase must be controlled. The second architecture of pulse generator consists in synthesizing UWB pulses with the help of digital circuits [11]. This type of pulse generator is more complex than other pulse generation methods since they are synthesized and not generated. It can theoretically address all particular UWB bands cutting [10] and also does not need a pulse shaping circuit to improve its frequency response. The synthesizing technique is well-suited for bipolar modulations but cannot permit high energy pulses to be generated due to low output dynamic. The third and last architecture is based on filter impulse response [4]. This generator has a simple architecture and can easily address a given frequency response since it consists in the excitation of a band pass filter. This kind of generator is principally used for bandwidth upper to 2GHz due to quality factor of integrated inductances [5]. Moreover, this topology is known for its low power potential [4] but is limited for BPSK modulation since it is difficult to drive the filter with perfect balanced signals [13].

In this paper, the design of a pulse generator for low-cost applications based on impulse filter response is presented. It can communicate in OOK, BPSK, or derivative of BPSK as AMI modulation and it is built for 3.1-4.9GHz, which corresponds to the fourth channel of the IEEE 802.15.4a standard, to maximize the power budget link of a transmission and to minimize the propagation loss. In the first part, the principle and the interest of using bipolar modulations is highlighted and demonstrated. The proposed architecture consists of a double pulse generator based on impulse filter

response and is described in section III. The section IV presents measurement results of the pulse generator realized in a ST-Microelectronics 130nm CMOS technology and a comparison with other UWB pulse generators conclude this paper.

II. Overview on Impulse Bipolar Modulations

In this section, a Pulse Amplitude Modulation (PAM), which is a particular case of Pulse Shape Modulation (PSM), is considered in order to demonstrate the interests of bipolar modulations as BPSK in terms of available energy by pulse, or bit rate. As shown on Fig. 1, the sequence voltage of pulses modulated in PAM s(t) can be written as follows:

$$s(t) = \sum_{k=0}^{K-1} d_k \cdot p\left(t - \frac{k}{D_S}\right) \tag{1}$$

where K is the number of emitted symbols in the sequence, p(t) the selected reference pulse according to the chosen f_M and BW_{-XdB}, D_S the symbol rate, and d_k the sequence of emitted symbols which are taken from the M-ary alphabet D. The alphabets which have to be taken into account in the next part are:

- $D_{OOK} : \{d_k\} = \{0,1\}$ for OOK,
- $D_{BPSK} : \{d_k\} = \{-1,1\}$ for BPSK.

A. Bipolar Modulations

By supposing that a modulated pulse sequence can be written as (1) and that the symbols of $\{d_k\}$ are not correlated between themselves, Bennett formula can be used to compute Power Spectral Density (PSD) $S_{ss}(f)$ of s(t) and can show the effects of the chosen modulation on the available bit rate [14]. It is also possible to write:

$$\begin{aligned} S_{ss}(f) &= D_S\left(E\left[D^2\right] - E[D]^2\right)\left|\hat{p}(f)\right|^2 \\ &\quad + {D_S}^2 E[D]^2 \left|\hat{p}(f)\right|^2 \delta_{D_S}(f) \end{aligned} \tag{2}$$

where :

- $\hat{p}(f)$ is the Fourier transform of p(t) in $V.Hz^{-1}$,
- $E[D]$ is the mean of D alphabet symbols $\{d_k\}$ during an infinite binary random sequence,
- $E[D]^2$ is the mean square of D alphabet symbols $\{d_k\}$ during an infinite binary random sequence,
- $\delta_{D_S}(f)$ is the Dirac comb with a 'period' of D_S.

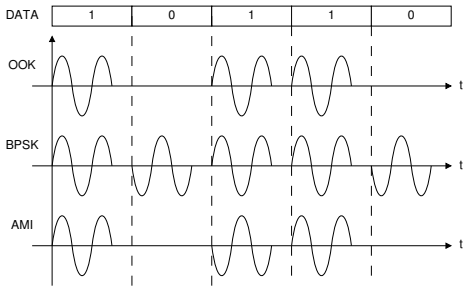

Figure 1. Principle of OOK, BPSK modulations in time domain.

This PSD can be linked with (i) the mean EIRP and the considered RBW at a given frequency f_0 with the help of an integral which gives:

$$EIRP(f_0) = \frac{1}{Z_L} \int_{f_0 - \frac{RBW}{2}}^{f_0 + \frac{RBW}{2}} S_{ss}(f) \cdot df \ . \tag{3}$$

with Z_L, the impedance load where the EIRP is measured. Equations (2) and (3) can be mixed and simplified by assuming that $\hat{p}(f)$ is constant equal to A^2 around the maximum emission frequency f_M which is a value directly proportional to pulse energy, f_M is a multiple of the symbol rate D_S, and D_S is upper than RBW. EIRP at f_M becomes then:

$$\begin{aligned} Z_L EIRP(f_M) &= D_S RBW\left(E\left[D^2\right] - E[D]^2\right)A^2 \\ &\quad + {D_S}^2 E[D]^2 A^2 \end{aligned} \ . \tag{4}$$

To demonstrate improvements due to the use of bipolar modulations, it is now necessary to compute $E[D^2]$ and $E[D]^2$ with the help of (5) and (6) which can be written as follows:

$$E[D]^2 = \left(\sum_{m=1}^{M} \Pr\left[d_k = d_{k,m}\right] \cdot d_{k,m}\right)^2 \tag{5}$$

and :

$$E\left[D^2\right] = \sum_{m=1}^{M} \Pr\left[d_k = d_{k,m}\right] \cdot {d_{k,m}}^2 \tag{6}$$

where $d_{k,m}$ is the m^{th} symbol of the M-ary alphabet D, and $\Pr[d_k = d_{k,m}]$ the probability to have the k^{th} emitted symbol d_k equal to $d_{k,m}$. As seen previously, M is equal to 2 for OOK, and BPSK modulations. $E[D^2]$ and $E[D]^2$ are also respectively equal to 1/2 and 1/4 for OOK modulation, 1 and 0 for BPSK modulation. It is now possible to write:

$$\begin{aligned} Z_L EIRP(f_M) &= \frac{1}{4} A^2 D_S\left(RBW + D_S\right) \text{ for OOK} \\ &= A^2 D_S \text{RBW} \qquad \text{for BPSK} \end{aligned} \tag{7}$$

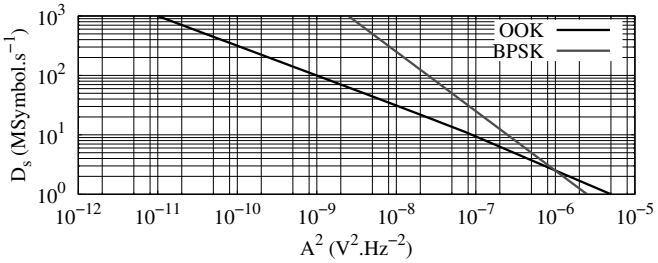

Figure 2. Available symbol rate for OOK, BPSK modulations.

which allows D_S versus A^2 to be plotted for each modulation on Fig. 2 for a given Z_L assumed to be equal to 50Ω, an EIRP equal to -41.3dBm and a RBW of 1MHz. It appears that for a given A^2, the authorized symbol rate by FCC is higher for BPSK modulations than OOK modulation while D_s is upper than 2MSymbol.s^{-1}. For a symbol rate of 30MSymbol.s^{-1}, the available energy that is possible to emit with BPSK modulation, is 10 times upper than the available power with OOK modulation. As a consequence, BPSK modulation allows also higher range to be achieved than OOK modulation.

Another particularity of IR-UWB communications is that it is possible to decrease (or increase) the emitted power in order to increase (or decrease) the symbol rate and inversely, always by respecting FCC rules.

B. Architectures for Bipolar Modulations

There are two ways to obtain architectures of pulse generators compliant with bipolar modulations. The most common way consists in the use of single-ended circuits thanks to its simplicity and the second is based on differential structures.

In this paper, the presented pulse generator is able to use bipolar modulations and is based on a duplicated single-ended circuit in order to keep advantages of single-ended circuits as a lower complexity and a single supply voltage. It keeps also advantages of differential structures as an high peak to peak output voltage.

III. BIPOLAR PULSE GENERATOR DESIGN

Architecture of the presented bipolar IR-UWB emitter is based on the excitation of two identical band-pass filters. The output signal s(t) is obtained by making a subtraction between the output signals of each filter called $s_1(t)$ and $s_2(t)$ as shown on Fig.3. The design of the proposed pulse generator can be cut in two parts. The first part consists of a double band-pass filter 3.1-4.9GHz and also FCC compliant, which have the particularity to be driven in current mode in order to optimize output dynamic on a 100Ω differential load. The second part is a baseband pulse generator which allows OOK, BPSK or AMI modulations to be done by generating shifted synchronized baseband pulses for band-pass filters integrated in the first part.

A. Double Filter Design

The both band pass filters are the same Bessel-Thompson filter. This type of filter is chosen thanks to its capability to generate the shortest pulses for a given bandwidth whereas its order is chosen equal to the lowest sufficient order to match the 3.1-4.9GHz band included in FCC mask. Advantages of low order filters, when they are integrated on a chip, are that they reduce the number of needed inductors and also reduce losses in the filter, and die area. However, the filter must be carefully designed to limit losses especially by reducing interconnect lengths during the step of the layout design. Next, the parasitic capacitances of each inductor must be compensated to avoid a degradation of the filter impulse response and ensure that generated pulses are not shifted in terms of frequency, and complies with the 3.1-4.9GHz band. Among the different possible filter structures, the chosen one offers many advantages. The first is that the resonator realized by L_1, L_2, and C_1 can be used to bias the filter driver and also allows the filter to be driven in current mode which increases the output peak to peak voltage. Each filter is also driven in a current mode by a class C amplifier based on Low Leakage MOS transistors in order to reduce leakage currents and also power consumption when no pulse is generated. Another important point is that the first resonator is based on two inductors L_1 and L_2 instead of a single inductor because it allows to reduce losses for the used technology. Next, C_s achieves a DC isolation. Finally, C_2 can be used to compensate pad capacitor and C_1, C_2, and C_P can be reduced to compensate some parasitic capacitors of L_1, L_P, and L_S.

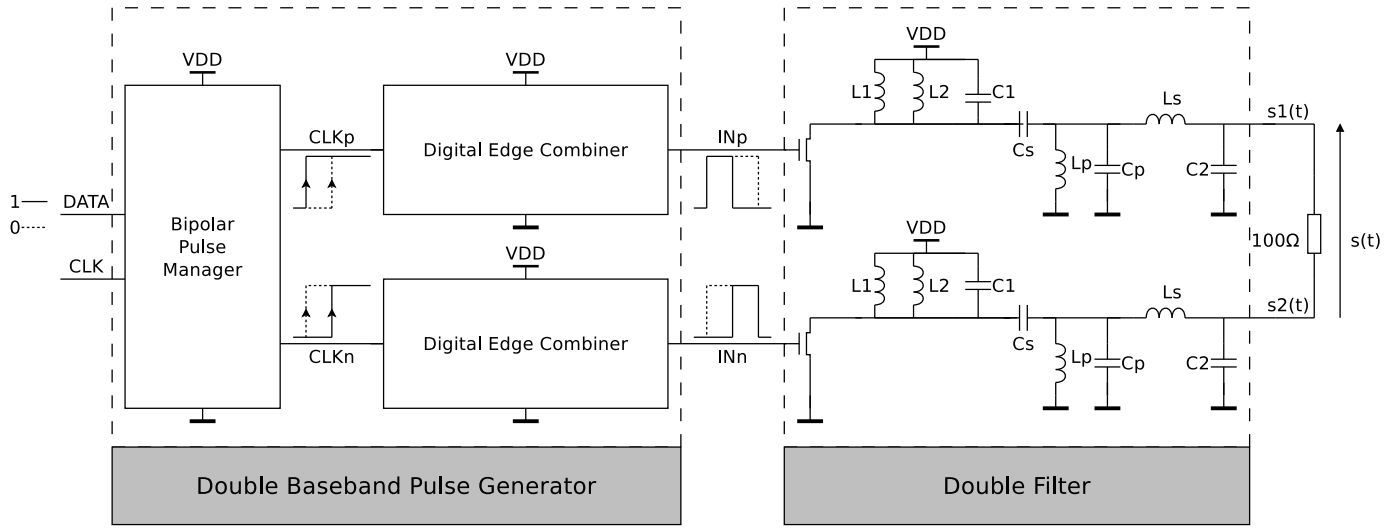

Figure 3. Principle of the proposed pulse generator.

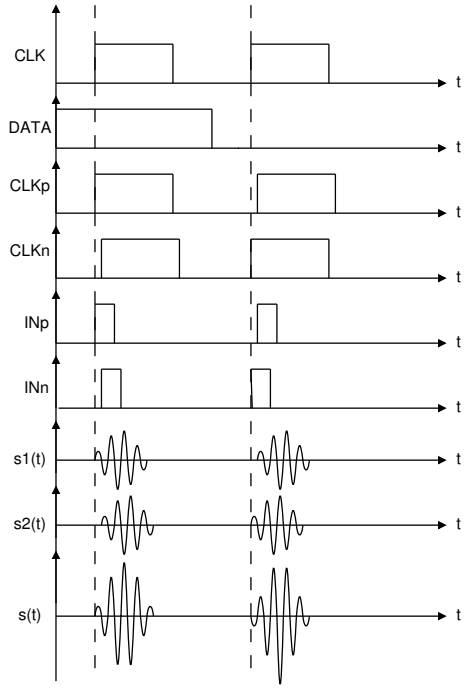

Figure 4. Main signals of the presented pulse generator in time domain.

B. *Double Baseband Pulse Generator Design*

The double baseband pulse generator is composed of two blocks. The first block is a bipolar pulse manager which allows bipolar modulations to be implemented and the second-one consists of two digital edge combiner driven by the first block. The bipolar pulse manager generates also one clock for each digital edge combiner called CLK_N and CLK_P. One of both clocks is always delayed of $1/(2f_M)$ which allow bipolar modulations to be obtained with two single ended filters. Thus, as shown on Fig. 4. CLK_N is delayed with a duration of $1/(2f_M)$ when DATA is equal to '1' and CLK_P is delayed with the same duration when DATA is equal to '0'. Next, digital edge combiner allows rising edge from CLK_N or CLK_P to be transformed in a baseband pulse respectively on IN_P or IN_N with a duration equal to $1/(2f_M)$, which allows maximum output dynamic to be obtained thanks to a delay line. To realize

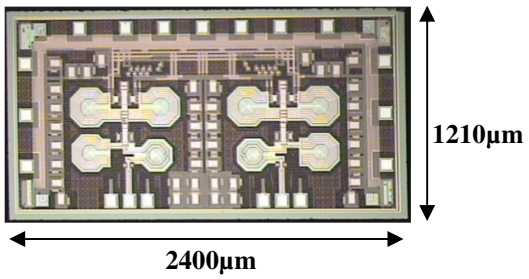

Figure 5. Chip micrograph of the proposed pulse generator.

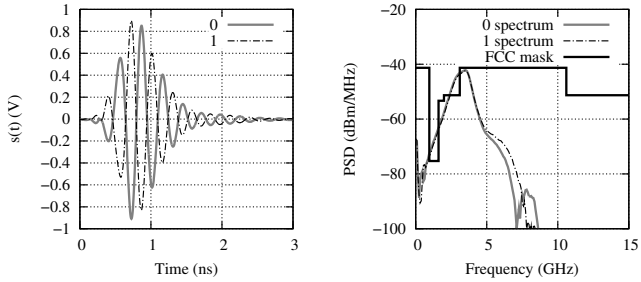

Figure 6. Measured responses of the presented pulse generator in time and frequency domains for DATA equal '0' and '1'.

this operation, two consecutive edges are combined to produce the baseband pulses required by filters with the help of a simple CMOS NOR gate. A driver based on inverter CMOS string is inserted at its output to match the small transistors used in the NOR gates with the large ones used in filters. Finally, one of both signals IN_P and IN_N are also delayed in function of the logic state of DATA and so, $s_1(t)$ and $s_2(t)$, are delayed too with the same conditions than IN_P and IN_N.

IV. MEASUREMENT RESULTS

The chip has been realized with a standard 130nm CMOS technology from ST-Microelectronics. As shown in Fig 5, the die area is about 2.88 mm². The measured responses of the pulse generator in time and frequency domains, which are shown in Fig. 6, demonstrate the pulse generator capability for bipolar modulations. Output peak to peak voltage is about 1.72Vpp on a 100Ω differential load and BW_{-10dB} is about 1.8GHz around 3.52GHz. However, the pulse generator is also 500MHz shifted regarding the initial desired center frequency which is equal to 4GHz. This shift is due to some inductive parasitic effects as the mutual inductor which are not take in account in post-layout simulations.

In a previous work [4], it has been demonstrated that the mean power consumption P_C is a function of the Pulse Repetition Frequency (PRF) and can be written as follows:

$$P_C(PRF) = E_{AC} \cdot PRF + P_{DC} \tag{8}$$

where P_{DC} is the constant DC power when no pulse is emitted and E_{AC} is the active energy added while a pulse is generated. In this work, the current consumption of the presented pulse generator when no pulse is emitted is equal to 100µA which leads to a P_{DC} of 120 µW with a voltage supply of 1.2V. The total power consumption P_C is equal to 0.513mW@1MHz and 4.05mW@10MHz. These values allow E_{AC} to be extracted and give an energy consumed by pulse of 393pJ/pulse. The emitted pulse energy E_p is equal to 1.93pJ.

TABLE I. PERFORMANCE SUMMARY OF PROPOSED GENERATOR AND COMPARAISON WITH PREVIOUS WORKS

[x]	V_{DD}	f_M	BW_{-10dB}	Vpp	Z_L	E_{AC}	P_{DC}	E_p	P_C@PRF	Correlation between bipolar pulses	MOD	DK	Method
	(V)	*(GHz)*	*(GHz)*	*(V)*	*(Ω)*	*(pJ/P)*	*(µW)*	*(pJ)*	*(mW)*			*(nm)*	
[13]	1.2	6	6.7	0.72	50	7.51	5818[a]	0.19[b]	7.32@200MHz	Bad	BPSK	130	Filter Response
[8]	1.2	4	4	0.35	50	NC	NC	0.08[b]	10@80MHz	Good	BPSK	130	Filter Response
[15]	1.2	4.5	1.2	0.9	50	175[a]	51.3[a]	1.69[b]	1.8@10MHz	Good	BPSK	180	OL Switching
[16]	1	3.5-4.5	0.5	0.71	50	271	137	2.52[b]	4.36@15MHz	Good	BPSK	90	Synthesizing
This work	1.2	3.52	1.8	1.72	100	393	120	2.05[b] 1.93[c]	4.05@10MHz	Good	BPSK	130	Filter Response

a. Estimated from published results - b. Approximated energy: $VPP^2/(8Z_L BW_{-10dB})$ - c. Real measured energy.

A comparison between some BPSK IR-UWB emitters is summarized in Table 1. It shows that this work allows bipolar modulations to be correctly implemented but also high energy pulses to be generated which is required to benefit of advantages of bipolar modulations in terms of bit rate and range. However, power consumption has to be improved which can be done by using techniques described in a previous work on a pulse generator based on impulse filter response [4].

V. CONCLUSION

The design of a pulse generator with an high output voltage for BPSK modulation has been presented. The topology has been carefully chosen to achieve pulses with an energy of 1.93pJ and a peak to peak voltage of 1.72V on a 100Ω differential load. Measurements demonstrate that the pulse generator can be used for bipolar modulation if off-chip elements as bond-wires or PCB lines are matched with cautions, thanks to a high intrinsic correlation between the both bipolar pulses. It also allows the communication range or the symbol rate to be higher than the ones possible with an identical pulse generator where OOK is only possible when FCC limitation is considered.

ACKNOWLEDGMENT

This work was carried out within the RUBY project which was supported by the French National Research Agency (ANR) and the Secured Communicating Solutions (SCS) world class cluster.

REFERENCES

[1] D. Lin, A. Trasser, H. Schumacher, "A Fully Differential IR-UWB Front-end for Noncoherent Communication and Localization," IEEE International Conference on Ultra-Wideband (ICUWB), 2011

[2] T. Yuan, Y. Zheng, C.W. Ang, L.W. Li, "A Fully Integrated CMOS Transmitter for Ultra-wideband Applications," Radio Frequency Integrated Circuits (RFIC) Symposium, IEEE, Page(s): 39-42, June 2007.

[3] S. Sim, D.W. Kim, S. Hong, "A CMOS UWB Pulse Generator for 6–10 GHz Applications," IEEE Microwave And Wireless Components Lettre, vol. 19, no. 2, Febuary 2009.

[4] R. Vauche, E. Bergeret, J. Gaubert, S. Bourdel, O. Fourquin, N. Dehaese, "A Remotely UHF Powered UWB Transmitter for High Precision Localization of RFID Tag," IEEE Internationnal Conference on Ultra-Wideband (ICUWB), 2011.

[5] S. Bourdel, Y. Bachelet, J. Gaubert, R. Vauche, O. Fourquin, N. Dehease, N. & H. Barthelemy, "A 9pJ/Pulse 1.42Vpp OOK CMOS UWB Pulse Generator for the 3.1-10.6 GHz FCC Band," IEEE Transaction on Microwave Theory and Techniques, vol. 58, no 1, Page(s): 65-73, January 2011.

[6] Y. Shamsa and W. A. Serdijn, "A 21pJ/pulse FCC Compliant UWB Pulse Generator," Circuits and Systems (ISCAS), Proceedings of 2010 IEEE International Symposium on, Page(s): 497 – 500, 2010.

[7] L. Zhou, Z. Chen, Student, C. C. Wang, F. Tzeng, V. Jain, P. Heydari, "A 2-Gb/s 130-nm CMOS RF-Correlation-Based IR-UWB Transceiver Front-End," IEEE Transaction On Microwave Theory And Techniques, vol. 59, no. 4, April 2011.

[8] L. Smaïni, C. Tinella, D. Hélal, C. Stoecklin, L. Chabert, C. Devaucelle, R. Cattenoz, N. Rinaldi, and D. Belot, "Single-Chip CMOS Pulse Generator for UWB Systems," IEEE Journal of Solid-State Circuits, vol. 41, no. 7, July 2006.

[9] Jeongwoo Han, Cam Nguyen, "Ultra-wideband electronically tunable pulse generators," in Microwave and Wireless Components Letters, IEEE, vol. 14, no 3, Page(s): 112-114, 2004.

[10] J. Han, C. Nguyen, "A New Ultra-Wideband, Ultra-Short Monocycle Pulse Generator With Reduced Ringing ," Microwave and Wireless Components Letters, IEEE Vol. 12 , no. 6, Page(s): 206 – 208, 2002.

[11] R. Vauche, S. Bourdel, N. Dehaese, O. Fourquin, J. Gaubert, "Fully Tunable UWB Pulse Generator with Zero DC Power Consumption," in Proc. IEEE Int. Conf. Ultra-Wideband ICUWB 2009, Page(s): 418-422, 2009.

[12] IEEE, "Part 15.4 : Wireless medium access control (mac) and physical layer (phy) specifications for low-rate wireless personal area networks (wpans)," 2007.

[13] Y. Bachelet, "Conception en technologie CMOS de générateurs d'impulsions Ultra Large Bande pour la norme américaine (FCC) et la norme européenne (ECC)," PhD thesis, Université d'Aix-Marseille I, 2008.

[14] R.Vauché, "Conception de générateur d'impulsion ultra-large bande en technologie CMOS," PhD thesis, Université de Provence, 2011

[15] D. Barras, F. Ellinger, H. Jäckel, W. Hirt, "Low-Power Ultra-Wideband Wavelets Generator With Fast Start-Up Circuit," IEEE Transactions on Microwave Theory and Technique, vol. 54, no5, May 2006.

[16] P. P. Mercier, D. C. Daly, A. P. Chandrakasan, "An Energy-Efficient All-Digital UWB Transmitter Employing Dual Capacitively-Coupled Pulse-Shaping Drivers," IEEE Journal of Solid-State Circuits, vol. 44, no. 6, June 2009.